THE WORLD JOURNAL OF BIOLOGICAL PSYCHIATRY
https://doi.org/10.1080/15622975.2020.1789217

ORIGINAL INVESTIGATION

An overview of the human brain myelin proteome and differences associated with schizophrenia

Daniel Martins-de-Souza[a,b,c,d], Paul C. Guest[a], Guilherme Reis-de-Oliveira[a], Andrea Schmitt[e], Peter Falkai[e] and Christoph W. Turck[f]

[a]Laboratory of Neuroproteomics, Department of Biochemistry and Tissue Biology, Institute of Biology, University of Campinas (UNICAMP), Campinas, Brazil; [b]Instituto Nacional de Biomarcadores em Neuropsiquiatria (INBION) Conselho Nacional de Desenvolvimento Científico e Tecnológico, São Paulo, Brazil; [c]Experimental Medicine Research Cluster (EMRC), University of Campinas, Campinas, Brazil; [d]D'Or Institute for Research and Education (IDOR), São Paulo, Brazil; [e]Department of Psychiatry and Psychotherapy, University Hospital, LMU Munich, Munich, Germany; [f]Department of Translational Research in Psychiatry, Max Planck Institute of Psychiatry, Munich, Germany

ABSTRACT

Objectives: Disturbances in the myelin sheath drive disruptions in neural transmission and brain connectivity as seen in schizophrenia. Here, the myelin proteome was characterised in schizophrenia patients and healthy controls to visualise differences in proteomic profiles.

Methods: A liquid chromatography tandem mass spectrometry-based shotgun proteomic analysis was performed of a myelin-enriched fraction of postmortem brain samples from schizophrenia patients ($n = 12$) and mentally healthy controls ($n = 8$). *In silico* pathway analyses were performed on the resulting data.

Results: The present characterisation of the human myelinome led to the identification of 480 non-redundant proteins, of which 102 proteins are newly annotated to be associated with the myelinome. Levels of 172 of these proteins were altered between schizophrenia patients and controls. These proteins were mainly associated with glial cell differentiation, metabolism/energy, synaptic vesicle function and neurodegeneration. The hub proteins with the highest degree of connectivity in the network included multiple kinases and synaptic vesicle transport proteins.

Conclusions: Together these findings suggest disruptive effects on synaptic activity and therefore neural transmission and connectivity, consistent with the dysconnectivity hypothesis of schizophrenia. Further studies on these proteins may lead to the identification of potential drug targets related to the synaptic dysconnectivity in schizophrenia and other psychiatric and neurodegenerative disorders.

ARTICLE HISTORY
Received 30 March 2020
Revised 11 June 2020
Accepted 22 June 2020

KEYWORDS
Oligodendrocytes; myelin; proteome; pathway; drug target

Introduction

The central role played by oligodendrocytes in myelination of neurons in the central nervous system (CNS) is essential for the proper functioning of the human brain. Myelin provides an electrically-insulating phospholipid layer, which facilitates the transmission of signal throughout axons, increases the speed of electrical impulses and avoids axonal electrical leakage. Naturally, disturbances in the myelin sheath may compromise the above-cited functions, affecting consequently neuronal and glial functions (Shimizu et al. 2018).

Oligodendrocyte-associated disturbances that directly affect myelination have been proposed as a pivotal feature in the pathogenesis of schizophrenia by different research groups, due to the critical role of these cells in the formation and maintenance of brain connectivity (Cassoli et al. 2016; Kolomeets and Uranova 2019). Such disturbances are proposed to originate at the neurodevelopmental level *in utero*, when the myelination process begins and then essentially terminates in early adulthood. This is because myelination must happen in biological harmony to construct and guide brain connectivity properly. This process may be disturbed by environmental factors or influenced by genetic variations (Dulamea 2017; Liu et al. 2019). Therefore, the characterisation of the molecular features of myelin in healthy and diseased human brains may

CONTACT Daniel Martins-de-Souza dmsouza@unicamp.br Laboratory of Neuroproteomics, Department of Biochemistry and Tissue Biology, Institute of Biology, University of Campinas (UNICAMP), Rua Monteiro Lobato, 255, Campinas, SP 13083-862, Brazil

Supplemental data for this article can be accessed at https://doi.org/10.1080/15622975.2020.1789217.

provide more precise insights about the biology of this structure and potential therapeutic targets.

Myelin is basically composed of lipids of well-characterised composition (Schmitt et al. 2015; Camargo et al. 2017; Li et al. 2017). However, characterising components involved in manufacturing and maintaining these structures at the protein level is also important for understanding myelin function in health and disease. The application of large-scale bottom-up shotgun proteomics can provide an overview of the protein composition in a qualitative and quantitative way (Becker and Bern 2011; Smith et al. 2019).

For a while now, researchers have been interested in the myelin proteome (referred to hereafter as myelinome) of the human brain. The first report of the human myelinome revealed 678 proteins (Ishii et al. 2009), followed by other two reports, which identified 770 proteins and 721 proteins (Dhaunchak et al. 2010; Gopalakrishnan et al. 2013). These reports provided insightful overviews of the human myelinome, serving as references – especially when Ishii and Dhaunchak compared human and murine myelinomes – from a qualitative point of view. These papers opened roads to the characterisation of the human myelinome in brain disorders.

In order to characterise the myelinome changes associated with schizophrenia, we macerated postmortem brain tissue (dorsolateral prefrontal cortex (DLPFC), Broadman Area 46) from mentally healthy donors and schizophrenia patients and then used a differential centrifugation technique to collect a myelin-enriched fraction (Dunkley et al. 1986). This fraction was homogenised and the protein content analysed by liquid chromatography tandem mass spectrometry-based shotgun proteomics (LC-MS/MS). The main objectives were to characterise the human myelinome of the cohort we are investigating and to identify any proteins belonging to the myelinome which were differentially regulated in schizophrenia.

Material and methods

Human brain tissue

Human brain samples were collected postmortem from 12 chronic schizophrenia patients and eight healthy controls. Detailed patient demographics are given in Supplementary Table 1. Patient samples were obtained at the Nordbaden Psychiatric Centre (Wiesloch, Germany), and healthy controls were collected at the Institute of Neuropathology, Heidelberg University (Heidelberg, Germany). All studied subjects were Germans, of white origin, with no history of alcohol or drug abuse. All analysed subjects were free from any somatic diseases and did not present any other brain degenerative disorder according to neuropathological characterisation (Braak staging lower than II) (Braak and Braak 1991). Brain samples were collected postmortem from mentally healthy individuals who had not taken antidepressants or antipsychotics during their lifetime. Schizophrenia patients had a record of antipsychotic treatment, so chlorpromazine equivalents (CPEs) could be calculated. The logarithmic CPE values show a normal distribution, with no outliers. Statistical analyses of patients' data suggest that our results are not biased towards demographics, as follows: (1) the postmortem interval median was 19 in patients, 17 in controls, $p = 0.9548$ (Mann–Whitney); (2) the brain pH median: 6.7 in patients, 6.6 in controls, $p = 0.9208$ (Mann–Whitney); (3) the median age: 67.5 in patients, 64.5 in controls, $p = 0.6921$ (Mann–Whitney); (4) gender: $p = 0.3729$ (Fisher's exact); (5) CPE median: 375. All evaluations and procedures were approved by the Ethics Committee of the Medical School of Heidelberg University. Patients and controls gave written consent for the use of their brains postmortem for research purposes.

Brain tissue myelin enrichment

Brain tissue was processed for myelin enrichment using a 4-step discontinuous Percoll gradient centrifugation technique as described in detail by Dunkley et al. (Dunkley et al. 1986). The efficacy of the myelin fraction enrichment can be verified in Figure 1(A). A fraction enriched in myelin biomarkers was collected from the 3/10% Percoll interface and homogenised in sodium dodecyl sulphate-polyacrylamide gel electrophoresis (SDS-PAGE) sample buffer (6% w/v SDS, 100 mM Tris pH 6.8, 30% glycerol, 100 mM dithiothreitol (DTT), 0.001% w/v bromophenol blue). Samples were diluted 10x and the protein content was estimated using the Bradford assay (Bradford 1976).

Western blot

Twenty micrograms of protein extracts from different fractions were loaded in a 12% SDS-PAGE and separated by electrophoresis (BioRad, Hercules, CA). Proteins were then transferred to Immobilon-FL polyvinyldiphenyl fluoride (PVDF) membranes (Millipore; Bedford, MA) at 100 V for 1 h with a cooling system. PVDF membranes were then soaked in 5% Carnation instant non-fat dry milk powder in Tris-buffered saline (pH 7.4) containing 0.1% Tween 20 (TBS-T) for 4 h. Next, membranes were rinsed in TBS-T three times for

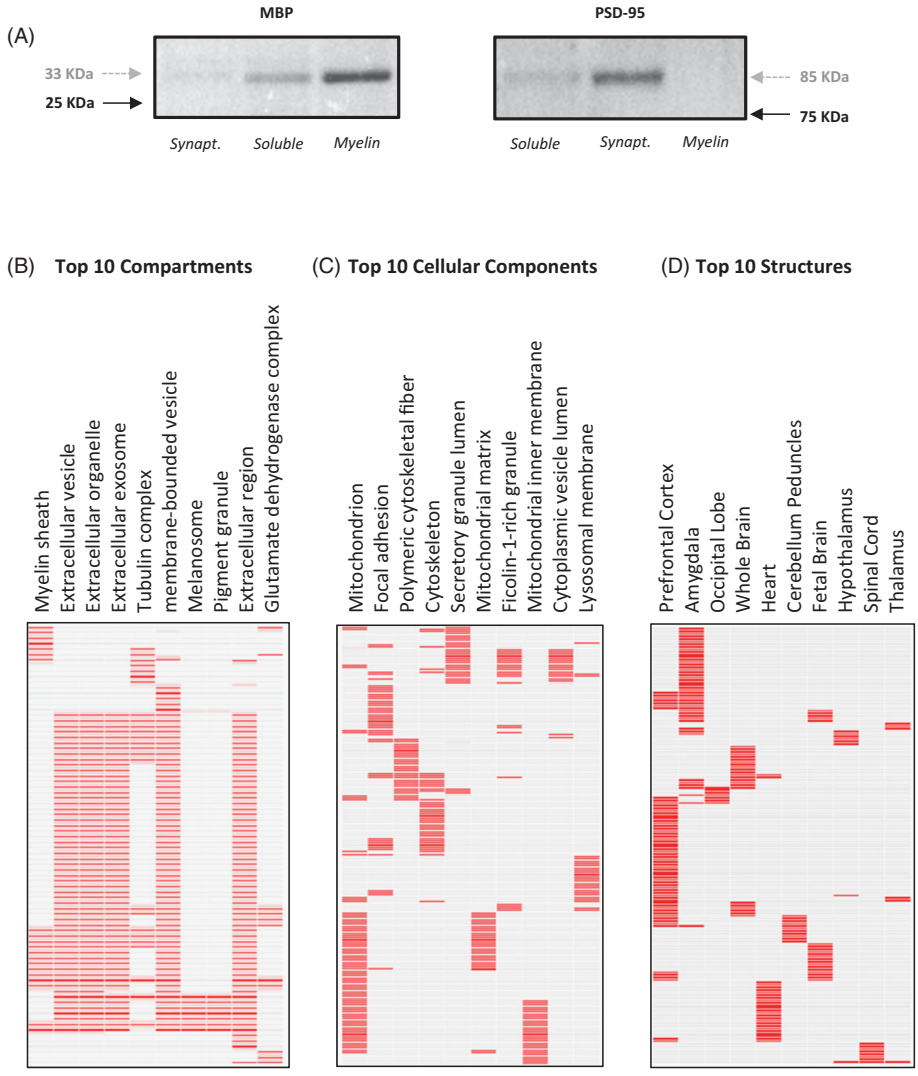

Figure 1. (A) Western blotting for the efficacy of the myelinome enrichment (PSD95: postsynaptic density protein 95 and MBP: myelin basic protein). In black are the ladder masses and in grey the expected masses. (B–D): EnrichR analysis of the myelinome showing enrichment of proteins associated with (B) cellular compartments, (C) cellular components, and (D) brain structures.

a total of 20 min, and incubated either with PSD95 (ab18258) or MBP (ab155995), at a dilution of 1:1000 in TBS-T overnight at 4 °C (antibodies were from Abcam, Cambridge, UK). Following the overnight incubation, membranes were rinsed twice with TBS-T for 15 min. Then, membranes were incubated with anti-c-MYC- peroxidase antibody 1:10,000 (GE Healthcare, Uppsala, Sweden) for 40 min at room temperature. Next, membranes were rinsed with water and TBS-T, and incubated with enhanced chemiluminescence (ECL) solution (GE Healthcare) for 1 min. The membranes were scanned using a ChemiDoc XRS+ (BioRad).

Sample preparation

We employed SDS-PAGE to purify proteins prior to LC-MS/MS analysis. Samples were boiled for 5 min and separated on in-house 12% bis-tris polyacrylamide gels polymerised using a standard protocol (Garcia et al. 2017). Samples were run for 5 min after having reached the separating gel (as indicated by the bromophenol blue dye front). A piece of each separated lane was cut from the top of the gel up to the dye front. The gel piece was diced then subjected to trypsin digestion *in situ* as described previously (Reis-de-Oliveira et al. 2019). The resulting peptides were lyophilised and frozen at −80 °C before LC-MS/MS analysis.

LC-MS/MS

Lyophilised peptides were suspended in an aqueous solution of 0.1% formic acid and injected into a nano-high-performance LC system (Eksigent, Dublin, CA,

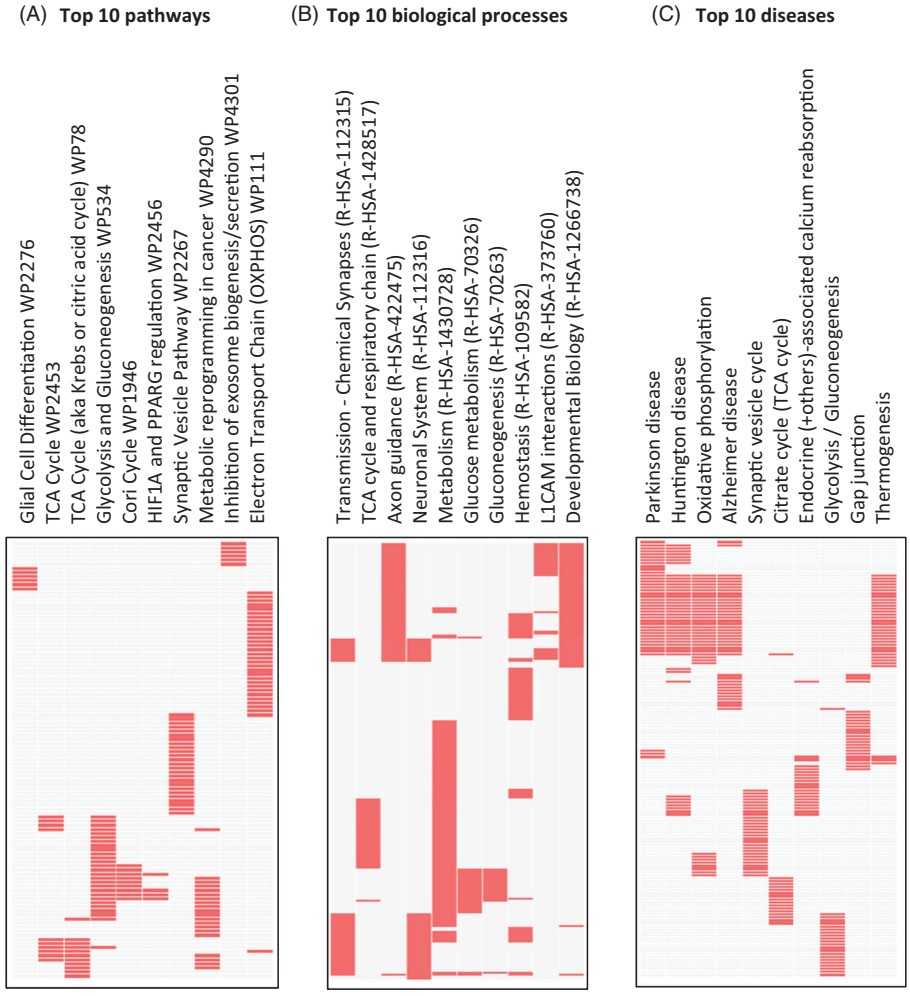

Figure 2. EnrichR analysis of the myelinome showing enrichment of proteins associated with (A) pathways, (B) biological processes, and (C) diseases.

USA) coupled to an LTQ XL-Orbitrap mass spectrometer (Thermo Scientific, Bremen, Germany). The peptides were separated using a discontinuous linear gradient from 98% solvent A (95% water, 5% acetonitrile, 0.1% formic acid) and 2% solvent B (99.9% acetonitrile, 0.1% formic acid) to 40% solvent A and 60% solvent B. Details on data acquisition are described in Maccarrone et al. (Maccarrone et al. 2014) using the following fragmentation parameters: repeat duration time, 30 s; isolation width, 2 mm; activation time, 30 ms; normalised collision energy, 35 V; and activation, Q = 0.250.

Proteomic data analysis

The resulting raw data were processed using MASCOT Distiller (Matrix Sciences, London, UK) for protein identification and quantification as previously described in detail (Saia-Cereda et al. 2017). For protein identification, we used the following criteria: peptide mass accuracy, 10 ppm; fragment ion mass accuracy, 0.5 Da; peptide false discovery rate (FDR), 1%; protein FDR, 1%; missed cleavages allowed, 2; enzyme, trypsin; fixed modification, cysteine carbamidomethylation; variable modification, methionine oxidation. Only proteins identified by at least 2 unique peptides were considered as part of the myelinome. Label-free spectral counting was employed for protein quantification. The cut-off criteria were set at a minimum of 5 MS/MS spectra for quantification. Proteins were considered differentially expressed if they were identified by at least 2 non-redundant peptides; presented a minimum fold change $\geq$1.5; a standard deviation of quantified peptides not greater than 10; and $p < 0.05$ (analysis of variance, ANOVA).

The myelinome and proteins differentially expressed between controls and schizophrenia patients were submitted to *in silico* systems biology analyses using Metascape (Zhou et al. 2019), EnrichR (Kuleshov et al. 2016) and ClusterProfiler (Yu et al. 2012) to identify the top 10 pathways, cellular compartments and diseases associated with the dataset.

The network of proteins associated with myelin sheath was generated in Cytoscape (Otasek et al. 2019). In addition, the differentially expressed protein dataset was analysed using the Search Tool for the Retrieval of Interacting Genes/Proteins (STRING) as an alternate means of identifying the most enriched pathways and hub proteins based on having the highest degrees of connectivity in the network (Szklarczyk et al. 2019). Finally, the total myelinome and differentially expressed protein datasets were compared using hierarchical clustering heat map analysis using Metascape as a means of determining which pathways were preferentially altered in schizophrenia.

Results

The human DLPFC myelinome

The DLPFC myelinome was properly enriched (Figure 1(A)) and initially characterised consisting of 629 unique proteins based on 4293 peptide identifications. After applying the basic filters for protein identification as detailed in the Methods section, 480 proteins remained and constituted the characterisation of the present human brain myelinome (Supplementary Table 2). The cellular compartments depicted by the presented myelinome confirmed myelin enrichment in the analysed sample (Figure 1(B)). As expected, the myelinome was also enriched in cellular components associated with energy production, structure and vesicular transport (Figure 1(C)). In addition, the myelinome was enriched in proteins originating from multiple brain structures (Figure 1(D)). Biological and biochemical processes enrichment showed that proteins comprising the myelinome-enriched fraction are involved in a number of biological processes such as glial cell differentiation, energy-associated pathways, synaptic vesicle cycle and axonal metabolism (Figure 2(A,B)). The proteins have previously been associated with brain diseases such as Parkinson's, Huntington's and Alzheimer's disease (Figure 2(C)).

The fold-change distribution of the myelinome shows the normality of the quantified data (Figure 3(A)). A number of the myelinome proteins constitute the myelin sheath and play diverse cellular roles (Figure 3(B)). De Monasterio-Schrader and colleagues (2012) performed a meta-analysis of the human brain myelinome, in which they describe 1200 proteins related to myelination and oligodendrocyte maturation (de Monasterio-Schrader et al. 2012). Our results show that 378 proteins identified in the DLPFC overlap with the meta-analysis performed by de Monasterio-Schrader, and 102 proteins are newly annotated to be associated with the myelinome (Figure 3(C)). In addition, when considering only human proteins, our study presents 160 new identities that constitute the myelin sheath in humans (Figure 3(D)). These 160 proteins are enriched for neuronal and energy-related cellular compartments (Figure 3(E)) and have been associated with several neurodegenerative disorders (Figure 3(F)).

Differences in the myelinome associated with schizophrenia

By performing relative quantitation of the myelinome, we found 172 proteins present at different levels between the schizophrenia and control myelinome fractions (Table 1). The top 20 biological processes enriched in the total myelinome were not similarly enriched in the top 20 biological processes of the differentially expressed proteins, as revealed by hierarchical clustering analysis (Figure 4). The finding that the processes of the latter were distinct from those in the total myelinome helped to discount the possibility of a technical bias related to the enrichment procedure. The biological processes represented in the myelinome and the differentially expressed protein subset, were grouped into major biological processes, providing a more general overview of the differences between the schizophrenia patients and controls. This is illustrated in Figure 5.

In terms of pathways, the differentially expressed proteins were mainly associated with glial cell differentiation, metabolism/energy, synaptic vesicle function and neurodegeneration (Figure 6(A)). At the level of cell compartments, these proteins were linked to the myelin structure, brain structure and vesicular transport systems (Figure 6(B)). Interestingly, the differentially expressed proteins showed enrichments in both psychiatric and degenerative diseases and the top represented disease was schizophrenia (Figure 6(C)).

The STRING analysis of the differentially expressed proteins (Figure 7) between control subjects and schizophrenia patients revealed that most of these proteins are involved in cellular processes associated with glial cell function, regulation of myelination, and neuronal cell differentiation and development. The hub proteins with the highest degree of connectivity were mitogen-activated protein kinase 1 (MAPK1), cell division control protein 42 homolog (CDC42), vesicle-associated membrane protein 2 (VAMP2), heat shock cognate 71 kDa protein (HSPA8), fibrinogen alpha chain (FGA), FGB, GTPase HRas (HRAS), clathrin

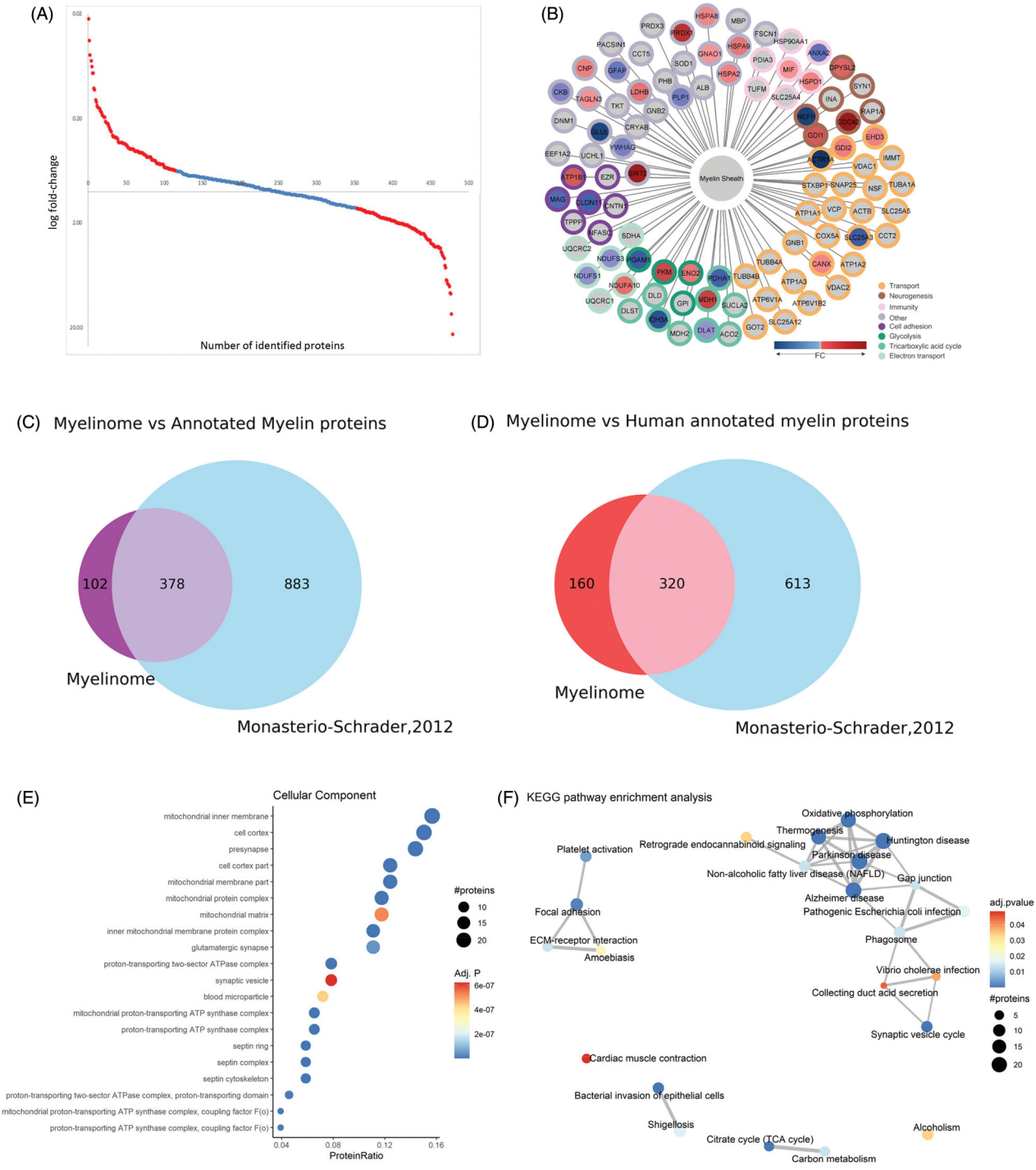

Figure 3. (A) Fold-change distribution of the myelinome: in red, those considered differentially expressed proteins. (B) Proteins of the myelinome which constitute the myelin sheath: proteins are outlined according to the biological processes they are involved in and the differentially expressed ones are coloured in red (upregulation) or blue (downregulated); (C-F): comparison between our findings and meta-analysis performed by de Monasterio-Schrader et al. (2012), considering proteins of (C) humans, mouse, and rat or (D) only human proteins. The 160 newly proteins described for humans were classified according to (E) cellular compartment and (F) pathway enrichment analyses.

light chain B (CLTB), clathrin coat assembly protein AP180 (SNAP91), dual specificity mitogen-activated protein kinase kinase 1 (MAP2K1), lamin-A/C (LMN), tropomyosin alpha-1 chain (TPM1), and heat shock 70 kDa protein 1 (HSPA1).

Discussion

While revealing 480 non-redundant proteins of the human myelinome, our study unites with the above-mentioned work of Ishii, Dhaunchak and

Table 1. Differentially expressed myelinome proteins.

UniProt ID	Gene Name	SZ/CT Ratio	# Peptides	Protein Name
CN37_HUMAN	CNP	1.89	45	2′,3′-cyclic-nucleotide 3′-phosphodiesterase OS = Homo sapiens GN = CNP PE = 1 SV = 2
PFKAL_HUMAN	PFKL	1.64	6	6-phosphofructokinase, liver type OS = Homo sapiens GN = B82 PE = 1 SV = 6
THIL_HUMAN	ACAT1	0.55	5	Acetyl-CoA acetyltransferase, mitochondrial OS = Homo sapiens GN = ACAT1 PE = 1 SV = 1
KAD1_HUMAN	AK1	1.91	2	Adenylate kinase isoenzyme 1 OS = Homo sapiens GN = AK1 PE = 1 SV = 3
CAP2_HUMAN	CAP2	3.47	3	Adenylyl cyclase-associated protein 2 OS = Homo sapiens GN = CAP2 PE = 1 SV = 1
ALDH2_HUMAN	ALDH2	1.59	6	Aldehyde dehydrogenase, mitochondrial OS = Homo sapiens GN = ALDH2 PE = 1 SV = 2
ACTN3_HUMAN	ACTN3	1.58	3	Alpha-actinin-3 OS = Homo sapiens GN = ACTN3 PE = 1 SV = 2
ACTZ_HUMAN	ACTR1A	0.07	2	Alpha-centractin OS = Homo sapiens GN = ACTR1A PE = 1 SV = 1
SYUA_HUMAN	SNCA	1.82	12	Alpha-synuclein OS = Homo sapiens GN = SNCA PE = 1 SV = 1
ANXA2_HUMAN	ANXA2	0.44	5	Annexin A2 OS = Homo sapiens GN = ANXA2 PE = 1 SV = 2
ANXA5_HUMAN	ANXA5	0.38	8	Annexin A5 OS = Homo sapiens GN = ANXA5 PE = 1 SV = 2
AATC_HUMAN	GOT1	1.57	12	Aspartate aminotransferase, cytoplasmic OS = Homo sapiens GN = GOT1 PE = 1 SV = 3
ATLA1_HUMAN	ATL1	0.66	5	Atlastin-1 OS = Homo sapiens GN = ATL1 PE = 1 SV = 1
E41L3_HUMAN	EPB41L3	0.54	13	Band 4.1-like protein 3 OS = Homo sapiens GN = EPB41L3 PE = 1 SV = 2
PGBM_HUMAN	HSPG2	0.06	7	Basement membrane-specific heparan sulphate proteoglycan core protein OS = Homo sapiens GN = HSPG2 PE = 1 SV = 3
SNAB_HUMAN	NAPB	3.38	9	Beta-soluble NSF attachment protein OS = Homo sapiens GN = NAPB PE = 2 SV = 2
SYUB_HUMAN	SNCB	1.98	6	Beta-synuclein OS = Homo sapiens GN = SNCB PE = 1 SV = 1
BASP1_HUMAN	BASP1	0.50	24	Brain acid soluble protein 1 OS = Homo sapiens GN = BASP1 PE = 1 SV = 2
PGCB_HUMAN	BCAN	2.51	8	Brevican core protein OS = Homo sapiens GN = BCAN PE = 1 SV = 2
CANB1_HUMAN	PPP3R1	4.17	2	Calcineurin subunit B type 1 OS = Homo sapiens GN = PPP3R1 PE = 1 SV = 2
CALM1_HUMAN	CALM1	2.04	9	Calmodulin OS = Homo sapiens GN = CALM1 PE = 1 SV = 2
CALX_HUMAN	CANX	1.79	5	Calnexin OS = Homo sapiens GN = CANX PE = 1 SV = 2
CALR_HUMAN	CALR	0.30	2	Calreticulin OS = Homo sapiens GN = CALR PE = 1 SV = 1
CAMKV_HUMAN	CAMKV	4.33	5	CaM kinase-like vesicle-associated protein OS = Homo sapiens GN = CAMKV PE = 2 SV = 2
KAPCB_HUMAN	PRKACB	0.37	2	cAMP-dependent protein kinase catalytic subunit beta OS = Homo sapiens GN = PRKACB PE = 1 SV = 2
KAP3_HUMAN	PRKAR2B	0.45	2	cAMP-dependent protein kinase type II-beta regulatory subunit OS = Homo sapiens GN = PRKAR2B PE = 1 SV = 3
CBR1_HUMAN	CBR1	3.22	8	Carbonyl reductase [NADPH] 1 OS = Homo sapiens GN = CBR1 PE = 1 SV = 3
CTNB1_HUMAN	CTNNB1	0.47	2	Catenin beta-1 OS = Homo sapiens GN = CTNNB1 PE = 1 SV = 1
CD9_HUMAN	CD9	1.63	5	CD9 antigen OS = Homo sapiens GN = CD9 PE = 1 SV = 4
CADM1_HUMAN	CADM1	0.42	3	Cell adhesion molecule 1 OS = Homo sapiens GN = CADM1 PE = 1 SV = 2
CADM2_HUMAN	CADM2	0.54	7	Cell adhesion molecule 2 OS = Homo sapiens GN = CADM2 PE = 2 SV = 1
CDC42_HUMAN	CDC42	4.00	2	Cell division control protein 42 homolog OS = Homo sapiens GN = CDC42 PE = 1 SV = 1
CDK5_HUMAN	CDK5	2.46	2	Cell division protein kinase 5 OS = Homo sapiens GN = CDK5 PE = 1 SV = 3
PDE2A_HUMAN	PDE2A	9.35	2	cGMP-dependent 3′,5′-cyclic phosphodiesterase OS = Homo sapiens GN = PDE2A PE = 1 SV = 1
AP180_HUMAN	SNAP91	2.02	2	Clathrin coat assembly protein AP180 OS = Homo sapiens GN = SNAP91 PE = 1 SV = 2
CLCA_HUMAN	CLTA	1.79	2	Clathrin light chain A OS = Homo sapiens GN = CLTA PE = 1 SV = 1
CLCB_HUMAN	CLTB	0.43	3	Clathrin light chain B OS = Homo sapiens GN = CLTB PE = 1 SV = 1
CLD11_HUMAN	CLDN11	0.34	3	Claudin-11 OS = Homo sapiens GN = CLDN11 PE = 1 SV = 2
CLUS_HUMAN	CLU	0.59	2	Clusterin OS = Homo sapiens GN = CLU PE = 1 SV = 1
CPLX2_HUMAN	CPLX2	3.32	3	Complexin-2 OS = Homo sapiens GN = CPLX2 PE = 1 SV = 2
KCRB_HUMAN	CKB	0.55	23	Creatine kinase B-type OS = Homo sapiens GN = CKB PE = 1 SV = 1
CAND1_HUMAN	CAND1	1.75	2	Cullin-associated NEDD8-dissociated protein 1 OS = Homo sapiens GN = CAND1 PE = 1 SV = 2
CSRP1_HUMAN	CSRP1	0.47	5	Cysteine and glycine-rich protein 1 OS = Homo sapiens GN = CSRP1 PE = 1 SV = 3
CYC_HUMAN	CYCS	0.41	9	Cytochrome c OS = Homo sapiens GN = CYCS PE = 1 SV = 2
COX2_HUMAN	MT-CO2	0.60	4	Cytochrome c oxidase subunit 2 OS = Homo sapiens GN = MT-CO2 PE = 1 SV = 1
COX6C_HUMAN	COX6C	1.85	3	Cytochrome c oxidase subunit 6C OS = Homo sapiens GN = COX6C PE = 1 SV = 2
DHPR_HUMAN	QDPR	3.15	3	Dihydropteridine reductase OS = Homo sapiens GN = QDPR PE = 1 SV = 2

(*continued*)

Table 1. Continued.

UniProt ID	Gene Name	SZ/CT Ratio	# Peptides	Protein Name
DPYL1_HUMAN	CRMP1	3.39	6	Dihydropyrimidinase-related protein 1 OS = Homo sapiens GN = CRMP1 PE = 1 SV = 1
DPYL2_HUMAN	DPYSL2	2.32	30	Dihydropyrimidinase-related protein 2 OS = Homo sapiens GN = DPYSL2 PE = 1 SV = 1
DNJC5_HUMAN	DNAJC5	3.77	2	DnaJ homolog subfamily C member 5 OS = Homo sapiens GN = DNAJC5 PE = 1 SV = 1
MP2K1_HUMAN	MAP2K1	0.62	3	Dual specificity mitogen-activated protein kinase kinase 1 OS = Homo sapiens GN = MAP2K1 PE = 1 SV = 2
DNM1L_HUMAN	DNM1L	0.44	2	Dynamin-1-like protein OS = Homo sapiens GN = DNM1L PE = 1 SV = 2
DYL1_HUMAN	DYNLL1	1.91	4	Dynein light chain 1, cytoplasmic OS = Homo sapiens GN = DYNLL1 PE = 1 SV = 1
EHD3_HUMAN	EHD3	1.86	2	EH domain-containing protein 3 OS = Homo sapiens GN = EHD3 PE = 1 SV = 1
EF1A1_HUMAN	EEF1A1	0.56	9	Elongation factor 1-alpha 1 OS = Homo sapiens GN = EEF1A1 PE = 1 SV = 1
ENDD1_HUMAN	ENDOD1	3.36	2	Endonuclease domain-containing 1 protein OS = Homo sapiens GN = ENDOD1 PE = 1 SV = 2
SH3G2_HUMAN	SH3GL2	1.71	4	Endophilin-A1 OS = Homo sapiens GN = SH3GL2 PE = 1 SV = 1
ENPL_HUMAN	HSP90B1	1.65	2	Endoplasmin OS = Homo sapiens GN = HSP90B1 PE = 1 SV = 1
EAA1_HUMAN	SLC1A3	0.22	6	Excitatory amino acid transporter 1 OS = Homo sapiens GN = SLC1A3 PE = 1 SV = 1
CAZA2_HUMAN	CAPZA2	2.57	2	F-actin-capping protein subunit alpha-2 OS = Homo sapiens GN = CAPZA2 PE = 1 SV = 3
FIBA_HUMAN	FGA	0.06	3	Fibrinogen alpha chain OS = Homo sapiens GN = FGA PE = 1 SV = 2
FIBB_HUMAN	FGB	0.07	4	Fibrinogen beta chain OS = Homo sapiens GN = FGB PE = 1 SV = 2
FIBG_HUMAN	FGG	0.04	5	Fibrinogen gamma chain OS = Homo sapiens GN = FGG PE = 1 SV = 3
FLNA_HUMAN	FLNA	0.35	8	Filamin-A OS = Homo sapiens GN = FLNA PE = 1 SV = 4
FLOT1_HUMAN	FLOT1	2.89	3	Flotillin-1 OS = Homo sapiens GN = FLOT1 PE = 1 SV = 3
LEG1_HUMAN	LGALS1	0.63	2	Galectin-1 OS = Homo sapiens GN = LGALS1 PE = 1 SV = 2
ENOG_HUMAN	ENO2	2.04	13	Gamma-enolase OS = Homo sapiens GN = ENO2 PE = 1 SV = 3
GDAP1_HUMAN	GDAP1	1.51	2	Ganglioside-induced differentiation-associated protein 1 OS = Homo sapiens GN = GDAP1 PE = 1 SV = 2
CXA1_HUMAN	GJA1	0.42	3	Gap junction alpha-1 protein OS = Homo sapiens GN = GJA1 PE = 1 SV = 2
GFAP_HUMAN	GFAP	0.47	40	Glial fibrillary acidic protein OS = Homo sapiens GN = GFAP PE = 1 SV = 1
GLNA_HUMAN	GLUL	0.19	5	Glutamine synthetase OS = Homo sapiens GN = GLUL PE = 1 SV = 4
GSTP1_HUMAN	GSTP1	1.59	2	Glutathione S-transferase P OS = Homo sapiens GN = GSTP1 PE = 1 SV = 2
RASH_HUMAN	HRAS	2.65	2	GTPase HRas OS = Homo sapiens GN = HRAS PE = 1 SV = 1
GBG3_HUMAN	GNG3	0.02	2	Guanine nucleotide-binding protein G(I)/G(S)/G(O) subunit gamma-3 OS = Homo sapiens GN = GNG3 PE = 2 SV = 1
GNAO_HUMAN	GNAO1	1.52	22	Guanine nucleotide-binding protein G(o) subunit alpha OS = Homo sapiens GN = GNAO1 PE = 1 SV = 4
GNAQ_HUMAN	GNAQ	3.38	5	Guanine nucleotide-binding protein G(q) subunit alpha OS = Homo sapiens GN = GNAQ PE = 1 SV = 3
HS71A_HUMAN	HSPA1A	1.78	8	Heat shock 70 kDa protein 1 OS = Homo sapiens G + B77N = HSPA1A PE = 1 SV = 5
HSP76_HUMAN	HSPA6	1.72	7	Heat shock 70 kDa protein 6 OS = Homo sapiens GN = HSPA6 PE = 1 SV = 2
HSP7C_HUMAN	HSPA8	1.78	22	Heat shock cognate 71 kDa protein OS = Homo sapiens GN = HSPA8 PE = 1 SV = 1
HSP72_HUMAN	HSPA2	1.85	13	Heat shock-related 70 kDa protein 2 OS = Homo sapiens GN = HSPA2 PE = 1 SV = 1
HPCL4_HUMAN	HPCAL4	1.92	3	Hippocalcin-like protein 4 OS = Homo sapiens GN = HPCAL4 PE = 2 SV = 3
HPLN2_HUMAN	HAPLN2	0.13	2	Hyaluronan and proteoglycan link protein 2 OS = Homo sapiens GN = HAPLN2 PE = 1 SV = 1
HPRT_HUMAN	HPRT1	3.11	3	Hypoxanthine-guanine phosphoribosyltransferase OS = Homo sapiens GN = HPRT1 PE = 1 SV = 2
IDH3A_HUMAN	IDH3A	0.25	10	Isocitrate dehydrogenase [NAD] subunit alpha, mitochondrial OS = Homo sapiens GN = IDH3A PE = 1 SV = 1
LDHB_HUMAN	LDHB	2.25	10	L-lactate dehydrogenase B chain OS = Homo sapiens GN = LDHB PE = 1 SV = 2
LMNA_HUMAN	LMNA	0.11	7	Lamin-A/C OS = Homo sapiens GN = LMNA PE = 1 SV = 1
LMNB2_HUMAN	LMNB2	0.17	3	Lamin-B2 OS = Homo sapiens GN = LMNB2 PE = 1 SV = 3
LSAMP_HUMAN	LSAMP	22.92	3	Limbic system-associated membrane protein OS = Homo sapiens GN = LSAMP PE = 1 SV = 2
MIF_HUMAN	MIF	1.56	2	Macrophage migration inhibitory factor OS = Homo sapiens GN = MIF PE = 1 SV = 4
PRIO_HUMAN	PRNP	14.69	2	Major prion protein OS = Homo sapiens GN = PRNP PE = 1 SV = 1

(*continued*)

Table 1. Continued.

UniProt ID	Gene Name	SZ/CT Ratio	# Peptides	Protein Name
MDHC_HUMAN	MDH1	2.92	7	Malate dehydrogenase, cytoplasmic OS = Homo sapiens GN = MDH1 PE = 1 SV = 4
MATR3_HUMAN	MATR3	0.35	2	Matrin-3 OS = Homo sapiens GN = MATR3 PE = 1 SV = 2
MGST3_HUMAN	MGST3	0.55	4	Microsomal glutathione S-transferase 3 OS = Homo sapiens GN = MGST3 PE = 1 SV = 1
MAP1A_HUMAN	MAP1A	0.34	4	Microtubule-associated protein 1A OS = Homo sapiens GN = MAP1A PE = 1 SV = 5
MARE2_HUMAN	MAPRE2	2.34	6	Microtubule-associated protein RP/EB family member 2 OS = Homo sapiens GN = MAPRE2 PE = 1 SV = 1
GHC2_HUMAN	SLC25A18	2.00	2	Mitochondrial glutamate carrier 2 OS = Homo sapiens GN = SLC25A18 PE = 2 SV = 1
TOM70_HUMAN	TOMM70	2.27	2	Mitochondrial import receptor subunit TOM70 OS = Homo sapiens GN = TOMM70A PE = 1 SV = 1
MK01_HUMAN	MAPK1	1.57	9	Mitogen-activated protein kinase 1 OS = Homo sapiens GN = MAPK1 PE = 1 SV = 3
CRYM_HUMAN	CRYM	1.59	3	Mu-crystallin homolog OS = Homo sapiens GN = CRYM PE = 1 SV = 1
BIN1_HUMAN	BIN1	0.61	5	Myc box-dependent-interacting protein 1 OS = Homo sapiens GN = BIN1 PE = 1 SV = 1
MYPR_HUMAN	PLP1	0.51	11	Myelin proteolipid protein OS = Homo sapiens GN = PLP1 PE = 1 SV = 2
MAG_HUMAN	MAG	0.38	2	Myelin-associated glycoprotein OS = Homo sapiens GN = MAG PE = 1 SV = 1
MOG_HUMAN	MOG	2.03	8	Myelin-oligodendrocyte glycoprotein OS = Homo sapiens GN = MOG PE = 1 SV = 1
MYL6_HUMAN	MYL6	0.36	2	Myosin light polypeptide 6 OS = Homo sapiens GN = MYL6 PE = 1 SV = 2
MYH9_HUMAN	MYH9	0.22	4	Myosin-9 OS = Homo sapiens GN = MYH9 PE = 1 SV = 4
MARCS_HUMAN	MARCKS	2.09	5	Myristoylated alanine-rich C-kinase substrate OS = Homo sapiens GN = MARCKS PE = 1 SV = 4
DDAH1_HUMAN	DDAH1	0.40	5	N(G),N(G)-dimethylarginine dimethylaminohydrolase 1 OS = Homo sapiens GN = DDAH1 PE = 1 SV = 3
SIR2_HUMAN	SIRT2	3.82	5	NAD-dependent deacetylase sirtuin-2 OS = Homo sapiens GN = SIRT2 PE = 1 SV = 2
NCAM2_HUMAN	NCAM2	0.41	3	Neural cell adhesion molecule 2 OS = Homo sapiens GN = NCAM2 PE = 1 SV = 2
NCALD_HUMAN	NCALD	0.59	3	Neurocalcin-delta OS = Homo sapiens GN = NCALD PE = 2 SV = 2
NCAN_HUMAN	NCAN	2.33	4	Neurocan core protein OS = Homo sapiens GN = NCAN PE = 2 SV = 3
NCDN_HUMAN	NCDN	0.42	4	Neurochondrin OS = Homo sapiens GN = NCDN PE = 1 SV = 1
NFH_HUMAN	NEFH	0.16	8	Neurofilament heavy polypeptide OS = Homo sapiens GN = NEFH PE = 1 SV = 4
NEUG_HUMAN	NRGN	2.04	2	Neurogranin OS = Homo sapiens GN = NRGN PE = 1 SV = 1
NEUM_HUMAN	GAP43	2.89	11	Neuromodulin OS = Homo sapiens GN = GAP43 PE = 1 SV = 1
GPM6A_HUMAN	GPM6A	2.26	11	Neuronal membrane glycoprotein M6-a OS = Homo sapiens GN = GPM6A PE = 1 SV = 2
NPTN_HUMAN	NPTN	0.41	5	Neuroplastin OS = Homo sapiens GN = NPTN PE = 1 SV = 1
NOE1_HUMAN	OLFM1	0.35	2	Noelin OS = Homo sapiens GN = OLFM1 PE = 1 SV = 4
NONO_HUMAN	NONO	0.20	2	Non-POU domain-containing octamer-binding protein OS = Homo sapiens GN = NONO PE = 1 SV = 4
OPCM_HUMAN	OPCML	9.50	2	Opioid-binding protein/cell adhesion molecule OS = Homo sapiens GN = OPCML PE = 1 SV = 1
PPIB_HUMAN	PPIB	2.51	3	Peptidyl-prolyl cis-trans isomerase B OS = Homo sapiens GN = PPIB PE = 1 SV = 2
PRDX1_HUMAN	PRDX1	3.20	4	Peroxiredoxin-1 OS = Homo sapiens GN = PRDX1 PE = 1 SV = 1
PGK1_HUMAN	PGK1	1.80	11	Phosphoglycerate kinase 1 OS = Homo sapiens GN = PGK1 PE = 1 SV = 3
PGAM1_HUMAN	PGAM1	0.30	11	Phosphoglycerate mutase 1 OS = Homo sapiens GN = PGAM1 PE = 1 SV = 2
PKP2_HUMAN	PKP2	0.05	2	Plakophilin-2 OS = Homo sapiens GN = PKP2 PE = 1 SV = 1
PROF2_HUMAN	PFN2	8.08	2	Profilin-2 OS = Homo sapiens GN = PFN2 PE = 1 SV = 3
PSA4_HUMAN	PSMA4	0.43	3	Proteasome subunit alpha type-4 OS = Homo sapiens GN = PSMA4 PE = 1 SV = 1
BSN_HUMAN	BSN	0.19	3	Protein bassoon OS = Homo sapiens GN = BSN PE = 1 SV = 4
NDRG2_HUMAN	NDRG2	2.41	4	Protein NDRG2 OS = Homo sapiens GN = NDRG2 PE = 1 SV = 2
NIPS2_HUMAN	NIPSNAP2	3.36	2	Protein NipSnap homolog 2 OS = Homo sapiens GN = GBAS PE = 1 SV = 1
PYC_HUMAN	PC	0.20	2	Pyruvate carboxylase, mitochondrial OS = Homo sapiens GN = PC PE = 1 SV = 2
ODPB_HUMAN	PDHB	0.41	6	Pyruvate dehydrogenase E1 component subunit beta, mitochondrial OS = Homo sapiens GN = PDHB PE = 1 SV = 3
KPYM_HUMAN	PKM	2.80	25	Pyruvate kinase isozymes M1/M2 OS = Homo sapiens GN = PKM2 PE = 1 SV = 4
GDIA_HUMAN	GDI1	2.53	17	Rab GDP dissociation inhibitor alpha OS = Homo sapiens GN = GDI1 PE = 1 SV = 2

(*continued*)

Table 1. Continued.

UniProt ID	Gene Name	SZ/CT Ratio	# Peptides	Protein Name
GDIB_HUMAN	GDI2	1.91	10	Rab GDP dissociation inhibitor beta OS = Homo sapiens GN = GDI2 PE = 1 SV = 2
PTPRZ_HUMAN	PTPRZ1	0.47	3	Receptor-type tyrosine-protein phosphatase zeta OS = Homo sapiens GN = PTPRZ1 PE = 1 SV = 4
RTN1_HUMAN	RTN1	2.71	5	Reticulon-1 OS = Homo sapiens GN = RTN1 PE = 1 SV = 1
AT2A2_HUMAN	ATP2A2	2.20	3	Sarcoplasmic/endoplasmic reticulum calcium ATPase 2 OS = Homo sapiens GN = ATP2A2 PE = 1 SV = 1
SEPT2_HUMAN	SEPTIN2	1.80	3	Septin-2 OS = Homo sapiens GN = SEPT2 PE = 1 SV = 1
SEPT5_HUMAN	SEPTIN5	0.50	11	Septin-5 OS = Homo sapiens GN = SEPT5 PE = 1 SV = 1
SEPT7_HUMAN	SEPTIN7	2.09	11	Septin-7 OS = Homo sapiens GN = SEPT7 PE = 1 SV = 2
PP2BA_HUMAN	PPP3CA	1.86	5	Serine/threonine-protein phosphatase 2B catalytic subunit alpha isoform OS = Homo sapiens GN = PPP3CA PE = 1 SV = 1
SFXN3_HUMAN	SFXN3	1.69	3	Sideroflexin-3 OS = Homo sapiens GN = SFXN3 PE = 2 SV = 1
AT1B1_HUMAN	ATP1B1	2.52	8	Sodium/potassium-transporting ATPase subunit beta-1 OS = Homo sapiens GN = ATP1B1 PE = 1 SV = 1
AT1B2_HUMAN	ATP1B2	0.26	3	Sodium/potassium-transporting ATPase subunit beta-2 OS = Homo sapiens GN = ATP1B2 PE = 1 SV = 3
S12A5_HUMAN	SLC12A5	0.62	3	Solute carrier family 12 member 5 OS = Homo sapiens GN = SLC12A5 PE = 2 SV = 3
GTR1_HUMAN	SLC2A1	0.64	2	Solute carrier family 2, facilitated glucose transporter member 1 OS = Homo sapiens GN = SLC2A1 PE = 1 SV = 2
SFRF3_HUMAN	SFRS3	0.34	2	Splicing factor, arginine/serine-rich 3 OS = Homo sapiens GN = SFRS3 PE = 1 SV = 1
STMN1_HUMAN	STMN1	1.58	12	Stathmin OS = Homo sapiens GN = STMN1 PE = 1 SV = 3
SUCA_HUMAN	SUCLG1	0.15	2	Succinyl-CoA ligase [GDP-forming] subunit alpha, mitochondrial OS = Homo sapiens GN = SUCLG1 PE = 1 SV = 4
SYN2_HUMAN	SYN2	2.06	11	Synapsin-2 OS = Homo sapiens GN = SYN2 PE = 1 SV = 3
SV2A_HUMAN	SV2A	1.93	5	Synaptic vesicle glycoprotein 2A OS = Homo sapiens GN = SV2A PE = 1 SV = 1
TCPD_HUMAN	CCT4	1.51	3	T-complex protein 1 subunit delta OS = Homo sapiens GN = CCT4 PE = 1 SV = 4
TCPZ_HUMAN	CCT6A	0.66	2	T-complex protein 1 subunit zeta OS = Homo sapiens GN = CCT6A PE = 1 SV = 3
PURA_HUMAN	PURA	0.40	2	Transcriptional activator protein Pur-alpha OS = Homo sapiens GN = PURA PE = 1 SV = 2
TAGL_HUMAN	TAGLN	0.66	4	Transgelin OS = Homo sapiens GN = TAGLN PE = 1 SV = 4
TAGL3_HUMAN	TAGLN3	1.59	2	Transgelin-3 OS = Homo sapiens GN = TAGLN3 PE = 1 SV = 2
TMOD2_HUMAN	TMOD2	1.99	2	Tropomodulin-2 OS = Homo sapiens GN = TMOD2 PE = 1 SV = 1
TPM1_HUMAN	TPM1	2.89	6	Tropomyosin alpha-1 chain OS = Homo sapiens GN = TPM1 PE = 1 SV = 2
TPM3_HUMAN	TPM3	2.01	7	Tropomyosin alpha-3 chain OS = Homo sapiens GN = TPM3 PE = 1 SV = 1
TPM2_HUMAN	TPM2	2.89	6	Tropomyosin beta chain OS = Homo sapiens GN = TPM2 PE = 1 SV = 1
TBA4A_HUMAN	TUBA4A	0.60	38	Tubulin alpha-4A chain OS = Homo sapiens GN = TUBA4A PE = 1 SV = 1
TBA8_HUMAN	TUBA8	0.63	22	Tubulin alpha-8 chain OS = Homo sapiens GN = TUBA8 PE = 1 SV = 1
TBB8_HUMAN	TUBB8	0.60	18	Tubulin beta-8 chain OS = Homo sapiens GN = TUBB8 PE = 1 SV = 2
VATD_HUMAN	ATP6V1D	2.14	2	V-type proton ATPase subunit D OS = Homo sapiens GN = ATP6V1D PE = 1 SV = 1
VATG2_HUMAN	ATP6V1G2	0.27	4	V-type proton ATPase subunit G 2 OS = Homo sapiens GN = ATP6V1G2 PE = 1 SV = 1
VATH_HUMAN	ATP6V1H	1.50	5	V-type proton ATPase subunit H OS = Homo sapiens GN = ATP6V1H PE = 1 SV = 1
VAMP2_HUMAN	VAMP2	3.49	4	Vesicle-associated membrane protein 2 OS = Homo sapiens GN = VAMP2 PE = 1 SV = 2
VAPA_HUMAN	VAPA	0.26	4	Vesicle-associated membrane protein-associated protein A OS = Homo sapiens GN = VAPA PE = 1 SV = 3
VGLU1_HUMAN	SLC17A7	1.57	5	Vesicular glutamate transporter 1 OS = Homo sapiens GN = SLC17A7 PE = 2 SV = 1
VIME_HUMAN	VIM	0.34	37	Vimentin OS = Homo sapiens GN = VIM PE = 1 SV = 4
VISL1_HUMAN	VSNL1	1.63	10	Visinin-like protein 1 OS = Homo sapiens GN = VSNL1 PE = 1 SV = 2

Gopalakrishnan, contributing to expanding the knowledge about the human brain myelinome. Our contribution comprises 102 novel myelinome proteins, in addition to 160 newly annotated proteins for human DLPFC. These proteins play a range of biological roles (Figure 3(E)) and enrich for pathways associated with several degenerative brain disorders as Alzheimer's, Parkinson's and Huntington diseases (Figure 3(F)).

In our study, the enrichment of specific cellular compartments, components and brain structures supports the validity of the isolation procedure, as does the Western blot shown in Figure 1(A). We have identified a number of mitochondrial proteins associated with metabolism and energy functions. Previous studies have suggested that mitochondria appear as a contaminant in purified myelin preparations (Taylor

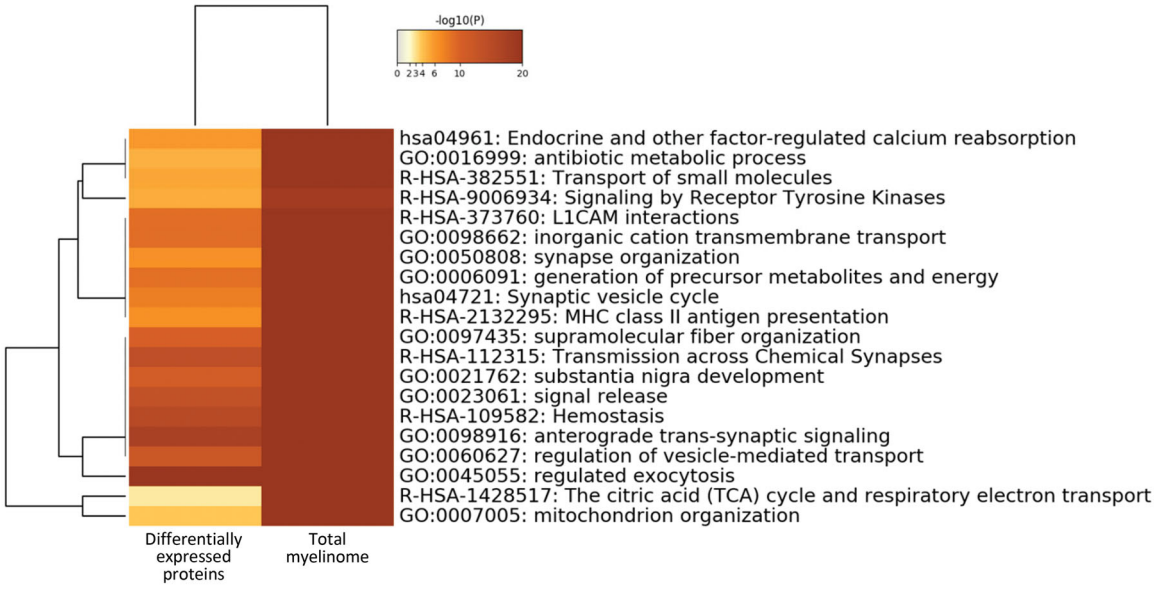

Figure 4. Hierarchical clustering analysis showing changes in proteins associated with specific pathways in the myelinome of schizophrenia patients relative to controls (by Metascape).

et al. 2004; Roth et al. 2006). Another research group hypothesised that myelin actually acts like a mitochondrion, by generating energy in the form of ATP across its membranes (Ravera et al. 2009). However, this proposal has been refuted by another study which suggested that if the respiratory chain was present in the myelin membranes, ATP synthase would function in reverse (Harris and Attwell 2013). Nevertheless, our finding that the human myelinome is also enriched with proteins associated with classical degenerative brain diseases such as Parkinson's, Huntington's and Alzheimer's disease, is consistent with the importance of myelin in these illnesses and highlights the specific proteins participating in this context.

All 'omic studies have the advantage over single target analyses through the potential identification of multiple genes or gene products associated with a molecular pathway. This enables the objective interpretation of the resulting data at the single molecule, molecular pathway and network levels, for a more comprehensive systems biology approach (Arrell and Terzic 2012). The over-representation of multiple genes in specific pathways or compartments in a particular dataset can also increase the validity of the findings. This process has been termed 'network biology' (Bensimon et al. 2012). In this study, *in silico* compartmentalisation of the brain structures associated with the myelinome allowed an integrated overview of the molecular processes involved in schizophrenia. Several of the biological processes and biochemical pathways we found to be associated with schizophrenia were previously observed in molecular studies, mainly in other proteomic studies of post-mortem brains (Martins-de-Souza et al. 2009a, 2009b; Chan et al. 2011; Deng et al. 2011; Martins-de-Souza 2011). This not only reinforces the roles of these processes in the disease, but also highlights the possibility that their function is disrupted in the myelin sheath.

Despite the limited information on the myelinome with regard to protein number, it seems clear that schizophrenia relevant pathways are part of it, reinforcing the current viewpoint that myelin, myelination and oligodendrocyte function play central roles in the disease (Raabe et al. 2019). In particular, data presented regarding the effects on glial cell function and differentiation, suggest that further attention should be paid to oligodendrocytes as a potential target for a new generation of antipsychotic medications.

The finding that several of the differentially expressed proteins in post-mortem myelinome were glycolysis enzymes, supports the fact that myelin function is tightly linked with metabolism and energy production pathways (Fünfschilling et al. 2012; Ravera et al. 2013). Previous studies have suggested that the whole energy machinery from glycolysis to the tricarboxylic acid cycle and oxidative phosphorylation are present in the vicinity of the myelin sheath (Ravera and Panfoli 2015). Not only is ATP produced there, but it appears that ATP and lactate are transported from the sheath to axons via connexins and monocarboxylate transporters. Thus, the differentially expressed proteins identified here support the hypothesis of dysfunctional energy production in schizophrenia (English et al. 2011; Gottschalk et al. 2015; Bryll et al. 2020),

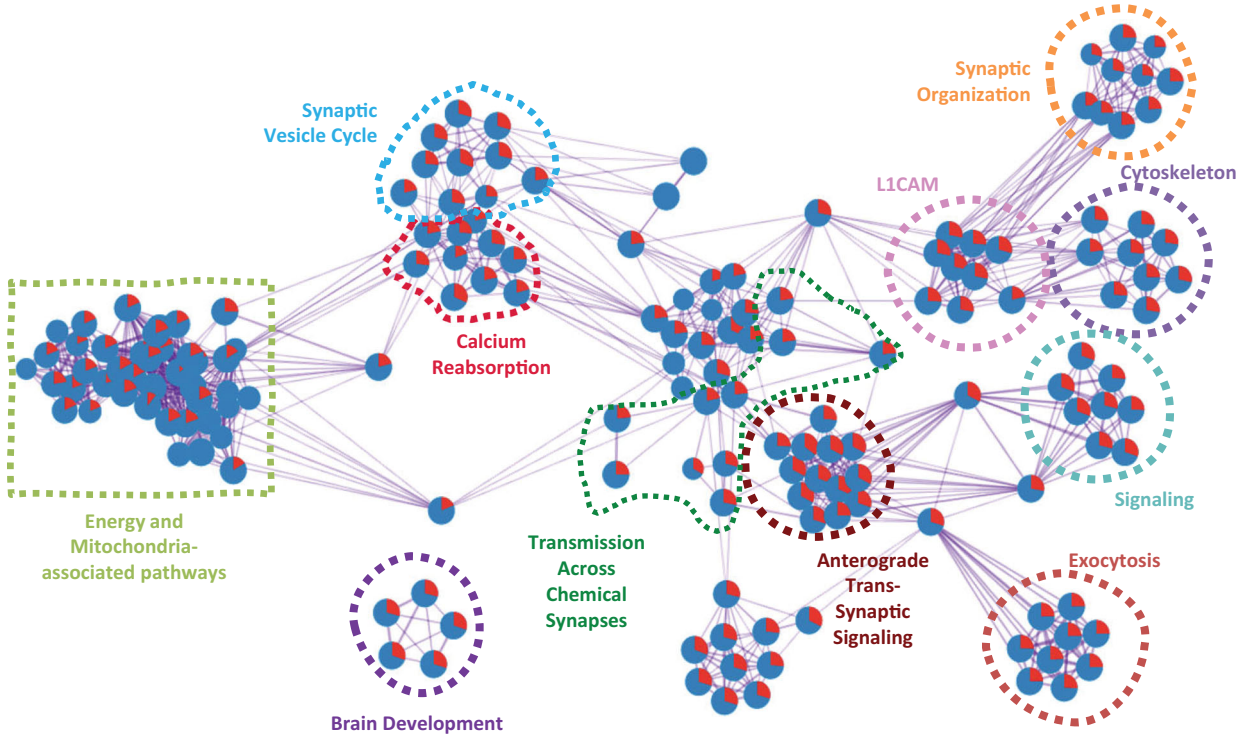

Figure 5. Biological processes associated with the differentially expressed protein subset between schizophrenia patients and controls (by Metascape).

and we suggest that at least part of these effects are apparent at the level of myelin sheath function.

2′,3′-Cyclic-nucleotide 3′-phosphodiesterase (CNP) is an oligodendrocyte-specific protein associated with early-phase maturation of these cells. Despite several studies having pointed to reduced CNP levels in schizophrenia (Flynn et al. 2003; Peirce et al. 2006; Reis-de-Oliveira et al. 2020), our results present that CNP is upregulated in the myelinome of these patients. Considering the role of antipsychotics over myelin-associated proteins, such upregulation might be related to the effect of medication (Ersland et al. 2017; Brandão-Teles et al. 2019). Additionally, the overexpression of CNP has been associated with imbalances in bipolar disorder (Hercher et al. 2014) and oligodendrocyte development (Gravel et al. 1996), which is a process affected in schizophrenia (Raabe et al. 2018). These findings suggest that CNP is a key protein for neuron and myelin homeostasis since alterations in its expression can lead to psychiatric disorders.

CNP is documented to interact with myelin basic protein (MBP) (Snaidero et al. 2017) during myelin sheath development and structure. Our results showed that MBP presented a modest upregulation in patients with schizophrenia (SZ/CT ratio = 1.23). The upregulation of MBP gene expression (Ota et al. 2019) was already documented in the DLPFC from patients with a first episode of psychosis; however, at the protein level, it remains controversial (Parlapani et al. 2009; Fernandez-Enright et al. 2014; Reis-de-Oliveira et al. 2020) when considering other brain regions or patient groups.

Proteolipid protein 1 (PLP1) is also a key protein in myelin formation, in which dysfunctions can lead to hypomyelinating leukodystrophy (Lossos et al. 2015). Our results show that PLP1 is downregulated in the DLPFC of patients with schizophrenia. This result is supported by other findings in the literature (Tkachev et al. 2003; Aston et al. 2004; Aberg et al. 2006), which documented a downregulation in PLP1 gene expression in psychiatric disorders. Despite mutations in PLP1 having been related to ataxia and cognitive impairments, it is still under debate whether these effects are linked to disease or medication side effects (Tkachev et al. 2003; Aberg et al. 2010).

Our finding of differential production of structural proteins (mainly tubulin complex, type-III intermediate filament, and proteins involved in neuronal projections) may indicate structural abnormalities associated with the myelin sheath in schizophrenia patients. It is well known that mechanotransduction, cytoskeletal rearrangements, activity-dependent myelination and maintenance of axons depend on the correct expression patterns of such proteins which are regulated by glial cells (Herbert and Monk 2017).

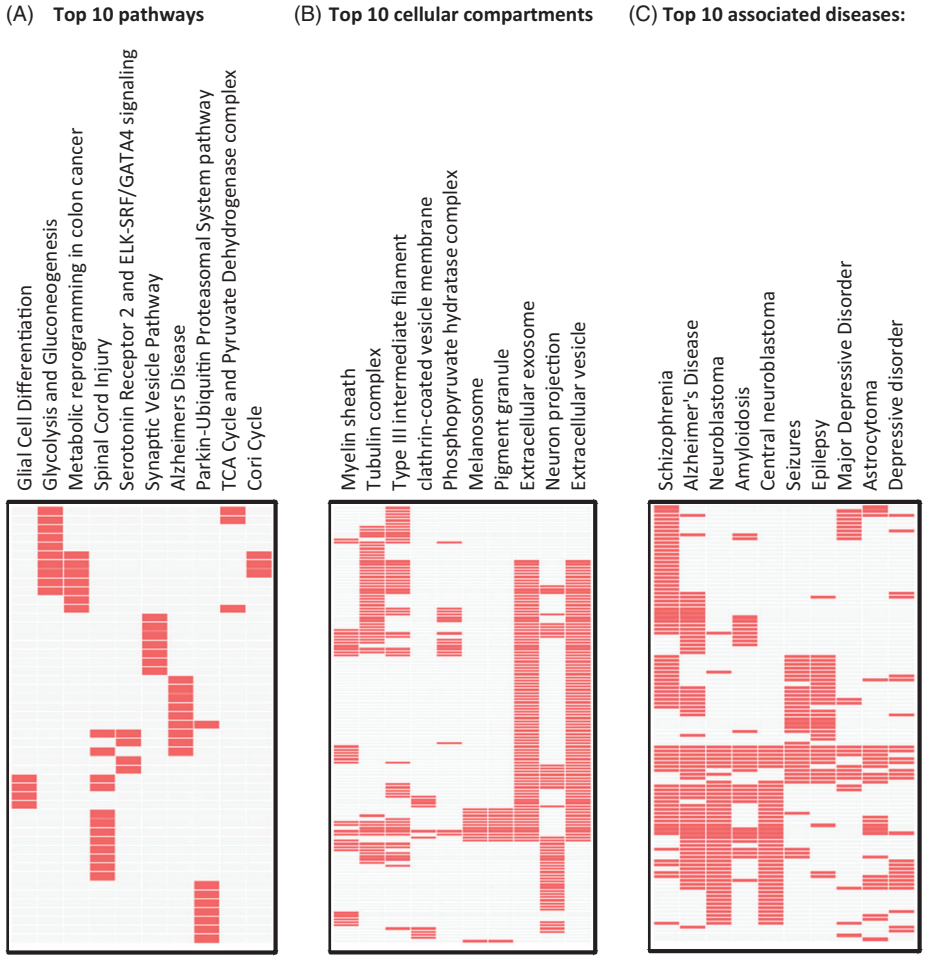

Figure 6. EnrichR analysis of the differentially expressed myelinome proteins showing enrichment of proteins associated with (A) pathways, (B) cellular compartments, and (C) diseases.

In addition, the altered expression of multiple proteins associated with transmission across chemical synapses, anterograde trans-synaptic signalling, exocytosis, and synaptic vesicle cycle and organisation in the schizophrenia myelinome, suggest disruptive effects on synaptic activity and therefore neural transmission and connectivity, are consistent with the dysconnectivity hypothesis of schizophrenia (van den Heuvel and Fornito 2014; Sun et al. 2016, 2017). Thus, further studies are warranted to investigate these proteins as potential biomarkers of synaptic dysconnectivity in schizophrenia and other psychiatric and neurodegenerative disorders.

Finally, the STRING analysis revealed several hub proteins that show a high degree of connectivity with other proteins in the myelinome. This included kinases (MAPK1 and MAP2K1), cell cycle proteins (CDC42), heat shock proteins (HSPA1 and HSPA8) and proteins involved in vesicle trafficking (HRAS, CLTB and SNAP91). These could represent key genes, signal pathways or therapeutic targets, which might help us improve our understanding of the pathophysiological mechanisms and identify new therapeutic agents for schizophrenia, related to myelin function.

There are a number of limitations to this study such as the use of post-mortem material with the possibility that the findings are due to artificial differences in brain structure, macromolecular integrity or even effect of antipsychotic medication (Crecelius et al. 2008). The study is also limited due to the small sample size, a fact that is often the case when working with human post-mortem tissue. Thus, replication of the findings is important. We suggest that validation studies are performed with more targeted techniques like selective reaction monitoring (SRM) to confirm the findings in other sample sets and appropriate preclinical models. Finally, despite the clear evidence that the myelin enrichment we performed was satisfactory (Figure 1(A)), the protocol we used here was originally developed for the isolation of synaptosomes. Other more specific protocols can also be used for the enrichment of myelin fraction (Ishii et al. 2018; Erwig et al. 2019).

Even though several of the biological processes that we have identified here have already been

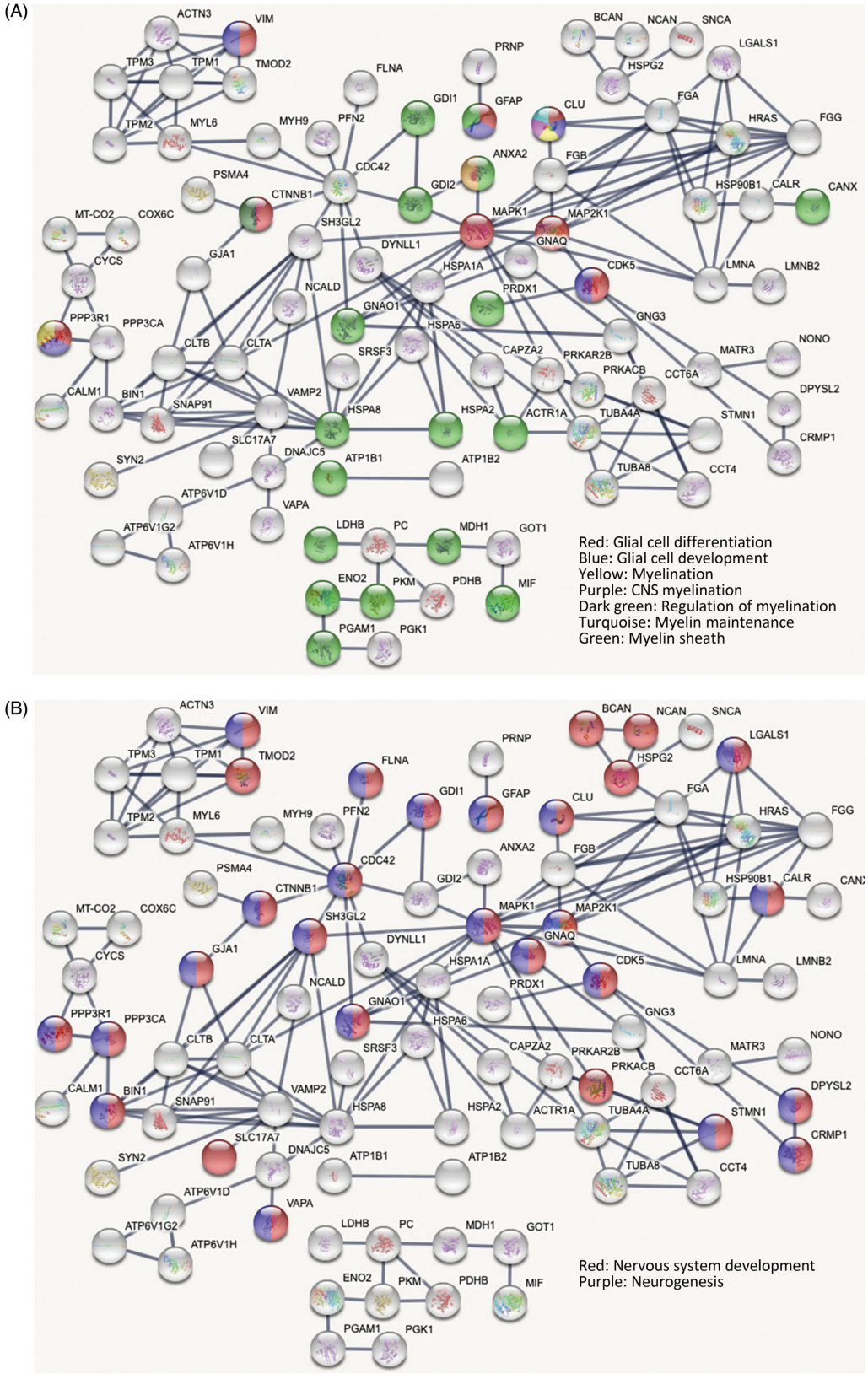

Figure 7. STRING analysis of the differentially expressed proteins between controls and schizophrenia patients revealing the most connected hub proteins and most enriched cellular processes focusing on (A) myelination and (B) neurodevelopment.

described as being associated with schizophrenia, we show for the first time that these biological processes and pathways are locally dysregulated at the level of the myelinome. This supports the concept of the

pivotal functioning of oligodendrocytes and the myelin sheath in schizophrenia pathogenesis. Thus, further studies should be performed as described above targeting the specific proteins and pathways identified in this study. The ultimate aim is to identify novel biomarkers and drug targets, which could pave the way for the development of new targeted therapeutic approaches for improved treatment of individuals suffering from this debilitating psychiatric disorder.

Acknowledgments

The authors dedicate this work to schizophrenia patients and mentally healthy donors, who understood the importance of their contribution to humankind.

Statement of interest

None to declare.

Funding

DMS and GRO are funded by São Paulo Research Foundation (FAPESP), grant 2017/25588-1, 2019/00098-7, and 2018/01410-1.

ORCID

Daniel Martins-de-Souza http://orcid.org/0000-0003-3595-5846
Paul C. Guest http://orcid.org/0000-0002-5030-7137
Andrea Schmitt http://orcid.org/0000-0002-5426-4023
Peter Falkai http://orcid.org/0000-0003-2873-8667

Data availability statement

Proteomic data that support the findings of this study are available from the corresponding author upon request.

References

Aberg K, Adkins DE, Bukszár J, Webb BT, Caroff SN, Miller DD, Sebat J, Stroup S, Fanous AH, Vladimirov VI, et al. 2010. Genomewide association study of movement-related adverse antipsychotic effects. Biol Psychiatry. 67: 279–282.

Aberg K, Saetre P, Jareborg N, Jazin E. 2006. Human QKI, a potential regulator of mrna expression of human oligodendrocyte-related genes involved in schizophrenia. Proc Natl Acad Sci USA. 103:7482–7487.

Arrell DK, Terzic A. 2012. Systems proteomics for translational network medicine. Circ Cardiovasc Genet. 5:478.

Aston C, Jiang L, Sokolov BP. 2004. Microarray analysis of postmortem temporal cortex from patients with schizophrenia. J Neurosci Res. 77:858–866.

Becker CH, Bern M. 2011. Recent developments in quantitative proteomics. Mutat Res. 722:171–182.

Bensimon A, Heck AJR, Aebersold R. 2012. Mass spectrometry-based proteomics and network biology. Annu Rev Biochem. 81:379–405.

Braak H, Braak E. 1991. Neuropathological stageing of Alzheimer-related changes. Acta Neuropathol. 82:239–259.

Bradford MM. 1976. A rapid and sensitive method for the quantitation of microgram quantities of protein utilizing the principle of protein-dye binding. Anal Biochem. 72: 248–254.

Brandão-Teles C, de Almeida V, Cassoli JS, Martins-de-Souza D. 2019. Biochemical pathways triggered by antipsychotics in human oligodendrocytes: potential of discovering new treatment targets. Front Pharmacol. 10:186.

Bryll A, Skrzypek J, Krzyściak W, Szelągowska M, Śmierciak N, Kozicz T, Popiela T. 2020. Oxidative-antioxidant imbalance and impaired glucose metabolism in schizophrenia. Biomolecules. 10:384.

Camargo N, Goudriaan A, van Deijk A-LF, Otte WM, Brouwers JF, Lodder H, Gutmann DH, Nave K-A, Dijkhuizen RM, Mansvelder HD, et al. 2017. Oligodendroglial myelination requires astrocyte-derived lipids. PLoS Biol. 15:e1002605.

Cassoli JS, Iwata K, Steiner J, Guest PC, Turck CW, Nascimento JM, Martins-de-Souza D. 2016. Effect of MK-801 and clozapine on the proteome of cultured human oligodendrocytes. Front Cell Neurosci. 10:52.

Chan MK, Tsang TM, Harris LW, Guest PC, Holmes E, Bahn S. 2011. Evidence for disease and antipsychotic medication effects in post-mortem brain from schizophrenia patients. Mol Psychiatry. 16:1189–1202.

Crecelius A, Götz A, Arzberger T, Fröhlich T, Arnold GJ, Ferrer I, Kretzschmar HA. 2008. Assessing quantitative post-mortem changes in the gray matter of the human frontal cortex proteome by 2-D DIGE. Proteomics. 8:1276–1291.

de Monasterio-Schrader P, Jahn O, Tenzer S, Wichert SP, Patzig J, Werner HB. 2012. Systematic approaches to central nervous system myelin. Cell Mol Life Sci. 69: 2879–2894.

Deng MY, Lam S, Meyer U, Feldon J, Li Q, Wei R, Luk L, Chua SE, Sham P, Wang Y, et al. 2011. Frontal-subcortical protein expression following prenatal exposure to maternal inflammation. PLoS One. 6:e16638.

Dhaunchak AS, Huang JK, De Faria Junior O, Roth AD, Pedraza L, Antel JP, Bar-Or A, Colman DR. 2010. A proteome map of axoglial specializations isolated and purified from human central nervous system. Glia. 58:1949–1960.

Dulamea AO. 2017. Role of oligodendrocyte dysfunction in demyelination, remyelination and neurodegeneration in multiple sclerosis. Adv Exp Med Biol. 958:91–127.

Dunkley PR, Jarvie PE, Heath JW, Kidd GJ, Rostas JA. 1986. A rapid method for isolation of synaptosomes on percoll gradients. Brain Res. 372:115–129.

English JA, Pennington K, Dunn MJ, Cotter DR. 2011. The Neuroproteomics of Schizophrenia. Biol Psychiatry. 69: 163–172.

Ersland KM, Skrede S, Stansberg C, Steen VM. 2017. Subchronic olanzapine exposure leads to increased expression of myelination-related genes in rat fronto-medial cortex. Transl Psychiatry. 7:1262.

Erwig MS, Hesse D, Jung RB, Uecker M, Kusch K, Tenzer S, Jahn O, Werner HB. 2019. Myelin: methods for purification and proteome analysis. Methods Mol Biol. 1936:37–63.

Fernandez-Enright F, Andrews JL, Newell KA, Pantelis C, Huang XF. 2014. Novel implications of lingo-1 and its signaling partners in schizophrenia. Transl Psychiatry. 4:e348.

Flynn SW, Lang DJ, Mackay AL, Goghari V, Vavasour IM, Whittall KP, Smith GN, Arango V, Mann JJ, Dwork AJ, et al. 2003. Abnormalities of myelination in schizophrenia detected in vivo with MRI, and post-mortem with analysis of oligodendrocyte proteins. Mol Psychiatry. 8:811–820.

Fünfschilling U, Supplie LM, Mahad D, Boretius S, Saab AS, Edgar J, Brinkmann BG, Kassmann CM, Tzvetanova ID, Möbius W, et al. 2012. Glycolytic oligodendrocytes maintain myelin and long-term axonal integrity. Nature. 485: 517–521.

Garcia S, Baldasso PA, Guest PC, Martins-de-Souza D. 2017. Depletion of highly abundant proteins of the human blood plasma: applications in proteomics studies of psychiatric disorders. In: Guest PC, editor. Multiplex biomarker techniques: methods and applications, methods in molecular biology. New York (NY): Springer. p. 195–204.

Gopalakrishnan G, Awasthi A, Belkaid W, De Faria O, Jr, Liazoghli D, Colman DR, Dhaunchak AS. 2013. Lipidome and proteome map of myelin membranes. J Neurosci Res. 91:321–334.

Gottschalk MG, Wesseling H, Guest PC, Bahn S. 2015. Proteomic enrichment analysis of psychotic and affective disorders reveals common signatures in presynaptic glutamatergic signaling and energy metabolism. Int J Neuropsychopharmacol. 18:pyu019.

Gravel M, Peterson J, Yong VW, Kottis V, Trapp B, Braun PE. 1996. Overexpression of 2′,3′-cyclic nucleotide 3′-phosphodiesterase in transgenic mice alters oligodendrocyte development and produces aberrant myelination. Mol Cell Neurosci. 7:453–466.

Harris JJ, Attwell D. 2013. Is myelin a mitochondrion? J Cereb Blood Flow Metab. 33:33–36.

Herbert AL, Monk KR. 2017. Advances in myelinating glial cell development. Curr Opin Neurobiol. 42:53–60.

Hercher C, Chopra V, Beasley CL. 2014. Evidence for morphological alterations in prefrontal white matter glia in schizophrenia and bipolar disorder. J Psychiatry Neurosci. 39: 376–385.

Ishii A, Dutta R, Wark GM, Hwang SI, Han DK, Trapp BD, Pfeiffer SE, Bansal R. 2009. Human myelin proteome and comparative analysis with mouse myelin. Proc Natl Acad Sci U S A. 106:14605–14610.

Ishii A, Han D, Bansal R. 2018. Proteomics analysis of myelin composition. Methods Mol Biol. 1791:67–77.

Kolomeets NS, Uranova NA. 2019. Reduced oligodendrocyte density in layer 5 of the prefrontal cortex in schizophrenia. Eur Arch Psychiatry Clin Neurosci 269:379–386.

Kuleshov MV, Jones MR, Rouillard AD, Fernandez NF, Duan Q, Wang Z, Koplev S, Jenkins SL, Jagodnik KM, Lachmann A, et al. 2016. Enrichr: a comprehensive gene set enrichment analysis web server 2016 update. Nucleic Acids Res. 44:W90–W97.

Li ZH, Lu FF, Shao Q, Zhu M, Cao L. 2017. [Progress in metabolism and function of myelin lipids]. Sheng Li Xue Bao. 69:817–829.

Liu S, Li A, Zhu M, Li J, Liu B. 2019. Genetic influences on cortical myelination in the human brain. Genes Brain Behavior. 18:e12537.

Lossos A, Elazar N, Lerer I, Schueler-Furman O, Fellig Y, Glick B, Zimmerman B-E, Azulay H, Dotan S, Goldberg S, et al. 2015. Myelin-associated glycoprotein gene mutation causes pelizaeus-merzbacher disease-like disorder. Brain. 138:2521–2536.

Maccarrone G, Lebar M, Martins-de-Souza D. 2014. Brain quantitative proteomics combining GeLC-MS and isotope-coded protein labeling (ICPL). Methods Molecul Biol. 1156: 175–185.

Martins-de-Souza D. 2011. Proteomics as a tool for understanding schizophrenia. Clin Psychopharmacol Neurosci. 9: 95–101.

Martins-de-Souza D, Gattaz WF, Schmitt A, Rewerts C, Maccarrone G, Dias-Neto E, Turck CW. 2009a. Prefrontal cortex shotgun proteome analysis reveals altered calcium homeostasis and immune system imbalance in schizophrenia. Eur Arch Psychiatry Clin Neurosci. 259:151–163.

Martins-de-Souza D, Gattaz WF, Schmitt A, Rewerts C, Marangoni S, Novello JC, Maccarrone G, Turck CW, Dias-Neto E. 2009b. Alterations in oligodendrocyte proteins, calcium homeostasis and new potential markers in schizophrenia anterior temporal lobe are revealed by shotgun proteome analysis. J Neural Transm. 116:275–289.

Ota VK, Moretti PN, Santoro ML, Talarico F, Spindola LM, Xavier G, Carvalho CM, Marques DF, Costa GO, Pellegrino R, et al. 2019. Gene expression over the course of schizophrenia: from clinical high-risk for psychosis to chronic stages. NPJ Schizophr. 5:5.

Otasek D, Morris JH, Bouças J, Pico AR, Demchak B. 2019. Cytoscape automation: empowering workflow-based network analysis. Genome Biol. 20:185.

Parlapani E, Schmitt A, Erdmann A, Bernstein H-G, Breunig B, Gruber O, Petroianu G, von Wilmsdorff M, Schneider-Axmann T, Honer W, et al. 2009. Association between myelin basic protein expression and left entorhinal cortex pre-alpha cell layer disorganization in schizophrenia. Brain Res. 1301:126–134.

Peirce TR, Bray NJ, Williams NM, Norton N, Moskvina V, Preece A, Haroutunian V, Buxbaum JD, Owen MJ, O'Donovan MC. 2006. Convergent evidence for 2′,3′-cyclic nucleotide 3′-phosphodiesterase as a possible susceptibility gene for schizophrenia. Arch Gen Psychiatry. 63:18–24.

Raabe FJ, Galinski S, Papiol S, Falkai PG, Schmitt A, Rossner MJ. 2018. Studying and modulating schizophrenia-associated dysfunctions of oligodendrocytes with patient-specific cell systems. NPJ Schizophr. 4:23.

Raabe FJ, Slapakova L, Rossner MJ, Cantuti-Castelvetri L, Simons M, Falkai PG, Schmitt A. 2019. Oligodendrocytes as a new therapeutic target in schizophrenia: from histopathological findings to neuron-oligodendrocyte interaction. Cells. 8:1496.

Ravera S, Bartolucci M, Calzia D, Aluigi MG, Ramoino P, Morelli A, Panfoli I. 2013. Tricarboxylic acid cycle-sustained oxidative phosphorylation in isolated myelin vesicles. Biochimie. 95:1991–1998.

Ravera S, Panfoli I. 2015. Role of myelin sheath energy metabolism in neurodegenerative diseases. Neural Regen Res. 10:1570–1571.

Ravera S, Panfoli I, Calzia D, Aluigi MG, Bianchini P, Diaspro A, Mancardi G, Morelli A. 2009. Evidence for aerobic ATP synthesis in isolated myelin vesicles. Int J Biochem Cell Biol. 41:1581–1591.

Reis-de-Oliveira G, Fioramonte M, Martins-de-Souza D. 2019. A complete proteomic workflow to study brain-related disorders via postmortem tissue. Methods in Molecular Biology (Clifton, N.J.). 1916:319–328.

Reis-de-Oliveira G, Zuccoli GS, Fioramonte M, Schimitt A, Falkai P, Almeida V, Martins-de-Souza D. 2020. Digging deeper in the proteome of different regions from schizophrenia brains. J Proteomics. 223:103814.

Roth AD, Ivanova A, Colman DR. 2006. New observations on the compact myelin proteome. Neuron Glia Biol. 2:15–21.

Saia-Cereda VM, Santana AG, Schmitt A, Falkai P, Martins-de-Souza D. 2017. The nuclear proteome of white and gray matter from schizophrenia postmortem brains. Mol Neuropsychiatry. 3:37–52.

Schmitt S, Cantuti Castelvetri L, Simons M. 2015. Metabolism and Functions of Lipids in Myelin. Biochim Biophys Acta. 1851:999–1005.

Shimizu T, Osanai Y, Ikenaka K. 2018. Oligodendrocyte-neuron Interactions: impact on myelination and brain function. Neurochem Res. 43:190–194.

Smith BJ, Martins-de-Souza D, Fioramonte M. 2019. A guide to mass spectrometry-based quantitative proteomics. Methods Molecular Biol. 1916:3–39.

Snaidero N, Velte C, Myllykoski M, Raasakka A, Ignatev A, Werner HB, Erwig MS, Möbius W, Kursula P, Nave K-A, et al. 2017. Antagonistic functions of MBP and CNP establish cytosolic channels in CNS myelin. Cell Rep. 18:314–323.

Sun Y, Chen Y, Lee R, Bezerianos A, Collinson SL, Sim K. 2016. Disruption of brain anatomical networks in schizophrenia: a longitudinal, diffusion tensor imaging based study. Schizophr Res. 171:149–157.

Sun Y, Dai Z, Li J, Collinson SL, Sim K. 2017. Modular-level alterations of structure-function coupling in schizophrenia connectome. Hum Brain Mapp. 38:2008–2025.

Szklarczyk D, Gable AL, Lyon D, Junge A, Wyder S, Huerta-Cepas J, Simonovic M, Doncheva NT, Morris JH, Bork P, et al. 2019. STRING V11: protein-protein association networks with increased coverage, supporting functional discovery in genome-wide experimental datasets. Nucleic Acids Res. 47:D607–D613.

Taylor CM, Marta CB, Claycomb RJ, Han DK, Rasband MN, Coetzee T, Pfeiffer SE. 2004. Proteomic mapping provides powerful insights into functional myelin biology. Proc Natl Acad Sci U S A. 101:4643–4648.

Tkachev D, Mimmack ML, Ryan MM, Wayland M, Freeman T, Jones PB, Starkey M, Webster MJ, Yolken RH, Bahn S. 2003. Oligodendrocyte dysfunction in schizophrenia and bipolar disorder. Lancet. 362:798–805.

van den Heuvel MP, Fornito A. 2014. Brain networks in schizophrenia. Neuropsychol Rev. 24:32–48.

Yu G, Wang LG, Han Y, He QY. 2012. ClusterProfiler: an R package for comparing biological themes among gene clusters. OMICS. 16:284–287.

Zhou Y, Zhou B, Pache L, Chang M, Hadj Khodabakhshi A, Tanaseichuk O, Benner C, Chanda SK. 2019. Metascape provides a biologist-oriented resource for the analysis of systems-level datasets. Nat Commun. 10:1523.